NACA RM L57K04

NACA

RESEARCH MEMORANDUM

INVESTIGATION OF VORTEX MOVEMENTS ABOUT A WING IN STEADY SUBSONIC FLOW UNDERGOING A LARGE ANGLE-OF-ATTACK CHANGE IN A BLAST-INDUCED GUST

By Donald R. McFarland and Paul W. Huber

Langley Aeronautical Laboratory
Langley Field, Va.

NATIONAL ADVISORY COMMITTEE
FOR AERONAUTICS

WASHINGTON

January 22, 1958
Declassified April 12, 1961

NACA RM L57K04

NATIONAL ADVISORY COMMITTEE FOR AERONAUTICS

RESEARCH MEMORANDUM

INVESTIGATION OF VORTEX MOVEMENTS ABOUT A WING IN STEADY SUBSONIC FLOW UNDERGOING A LARGE ANGLE-OF-ATTACK CHANGE IN A BLAST-INDUCED GUST

By Donald R. McFarland and Paul W. Huber

SUMMARY

Measurements of the vortex movements with time about an airfoil undergoing a blast of sufficient strength to exceed momentarily the stall angle by a large amount have been made. For simulated subsonic flight it was found that the leading-edge vortex chordwise movement was closely similar to the chordwise load peak movement of a free-flight model twenty times as large previously reported at similar flight and blast conditions. No effect of leading- or trailing-edge radius on the vortex movements was noted for these conditions, and this result also suggests little or no effect of scale. In addition to the measurements for the flight-simulated case, measurements were obtained without flight simulation but with blast orientation and strength such as to produce the same maximum resultant angle of attack and velocity.

For both cases investigated, the vortex movements in general appear to be dependent on the fluid movement about the vortex, with little or no direct effect of blast-wave orientation noted. The leading-edge vortex was found to move at one-third to one-half of the free-stream fluid velocity, and the trailing-edge vortex to move at about the free-stream velocity. It is shown that cases which exhibit a different timewise dependency of the fluid movement with respect to a body likewise exhibit a different timewise dependency of the vortex movement or loading with respect to the body.

Comparison of pertinent results with a theory by Rott, applicable to shock-tube flow, yielded good agreement when an alteration to the theory was made to apply to the quasi-steady conditions.

INTRODUCTION

The importance of understanding the flow about an airfoil undergoing a sudden change in angle of attack is seen from the large changes in loading of an aircraft wing that can occur in flight involving a blast-induced gust. In reference 1, the actual loading as a function of time over the wing of an aircraft model in flight involving blast-induced gust was measured for the case of the blast normal to the airfoil and arriving from the under side. It was found from the chordwise loading change with time that a large load peak (that is, lifting pressure) was formed at the leading edge of the wing at the time of encounter and that this peak swept downstream over the upper surface of the wing at about one-third the forward velocity of the model. The magnitude of the blast-induced gust in this case was such that the initial angle-of-attack change was an increase to well above the steady-flow stall angle. The magnitude of the load peak was greater than could be accounted for even by potential flow calculations for the chordwise location of the load peak and wing attack angle. Although this load peak was not actually observed to be a vortex, the premise was advanced that such a vortex probably was formed and accounted for the observed load variations. In connection with this same type of problem, the loading on a double-wedge airfoil mounted in a shock tube at an angle of attack to the shock-tube flow was studied interferometrically as a function of time (ref. 2). These tests were conducted at angles up to the steady-flow stall angle of the airfoil but not greatly exceeding this angle. No moving load peak was evident from the computed surface pressure distributions nor was a moving vortex evident from the interferograms. Changes in the loading with time that were quite different in character from the free-flight results of reference 1 were observed, but in this case also the lift in the earlier stages of encounter was higher than could be accounted for on the basis of steady-flow tunnel data. In reference 3 interferograms are presented for a rounded-nose airfoil in a shock tube at an angle of attack well below the stall angle. Loads were not computed nor were vortices formed at the leading edge of the airfoil.

Previous shock-tube investigations of the diffraction of shock waves about objects of various shapes have shown that large, well-defined vortices may be formed under many conditions (refs. 3, 4, 5, and 6). These conditions involve the sudden turning or acceleration of fluid about corners and bends as a result of the shock diffraction about these turns. Prior to the shock-wave movement over these objects in the shock tube, there is, of course, no air flow, air-flow direction, or pressure field about the objects to enable the oncoming shock and shock-induced flow to be influenced by the shape of the object until it is actually encountered. At the time of shock arrival the flow field must be rather abruptly established by means of wave movements (that is, diffraction of both

shock and expansion waves set up by the object). Since wave movements in such a diffraction situation are generally faster than the fluid movements, an additional time after this wave diffraction time is then required for the fluid movements to engulf the objects and finally establish steady flow in the case of shock-tube investigations (refs. 2, 7, and 8). The final steady pattern usually shows regions of separation starting from the points at which the vortices originated. The vortices have, of course, moved downstream out of the flow field.

The speed of movement of such a vortex is described in a theory by Rott (found in ref. 6) for the case of a wedge in a shock tube. This theory indicates that the velocity of the center of the vortex is a function of the shock strength, the wedge angle, the angle of attack of the wedge, and the angle between the vortex path and the wedge surface. An isentropic theory developed by Howard (ref. 6) describes the variation, from the center of the vortex, of density, tangential velocity, and radial velocity. Howard's theory gives good agreement with his interferometric measurements, and his rate of growth of the vortex agrees with Rott's vortex velocity. Both theories require the insertion of an experimentally determined boundary condition.

As yet, however, the actual mechanism by which the vortex is formed is not clearly understood. It cannot be said from shock-tube studies whether the vortex is the result of shock-wave diffraction in itself, or more logically whether the vortex formation results from inability of the induced flow to complete the turn, with shock diffraction being merely a means for turning the flow in these cases. The inability to resolve the causes in shock-tube studies arises simply from the fact that the local induced flow direction is the same as the local direction of wave movement.

In the case of an aircraft in flight encountering a blast-induced gust, the resultant quasi-steady air flow over the aircraft does not necessarily have the same direction as the blast-wave movement but rather depends upon the forward velocity of the aircraft and the blast-wave strength as well as the blast-wave direction of movement. It is then possible in flight to encounter a blast such that the resultant flow direction is quite different from the direction of blast-wave movement. Also, in the case of aircraft there is an initial flow field about the body which consists of the viscous layers (boundary layer and wake) superimposed on the potential field, both of which might have some degree of influence upon the development of the transient flow pattern. A third difference between the conditions existing in flight through a blast and in shock-tube studies is seen in the expansion-wave part of the blast - that is, the part following the front (shock wave) of the blast. In this part of the blast a difference in character of the timewise variation of resultant velocity and angle of attack is found.

In order to provide a better understanding of the vortex movements about an airfoil under flight conditions such as were encountered in reference 1, an optical investigation was conducted on the blast-wave table of the Langley gas dynamics laboratory using a 1/20-scale section of the model wing used in reference 1. In this investigation the vortex movements with time under simulated free-flight conditions were clearly observable from timed schlieren photographs.

SYMBOLS

a	velocity of sound
b	exponent in equation (A1)
c	airfoil chord
l	distance parameter in blast-wave flow (see appendix A)
M	flow Mach number $\left(\frac{u}{a}\right)$
n	wedge-angle function $\left(\frac{\pi}{2\pi - \epsilon}\right)$
p	pressure, lb/sq in. abs
r	distance from vortex to point of origin
t	time from shock encounter with a specified point, $t = 0$ at $l = 0$ or at $r = 0$, microseconds
t'	time during which there has been shock-induced flow at any fixed point
t_d	time duration at a fixed point of positive overpressure in blast
u	fluid-flow velocity, ft/sec
u_e	equivalent-flow velocity (see eq. 3)
V	shock-wave velocity (blast front)
x	free-stream flow displacement in a chordwise direction
y	free-stream flow displacement in direction normal to chord

α angle of attack of airfoil, deg

β angle between line connecting vortex and its origin with airfoil mean line

ϵ wedge angle

γ ratio of specific heats

Subscripts:

0 initial flow ($t < 0$)

2 blast flow immediately behind shock wave

B blast flow

R resultant of blast and initial components

X in a chordwise direction

Y in a direction normal to the chord

APPARATUS

The apparatus used for these experiments was the blast-wave table of the Langley gas dynamics laboratory described in reference 9, modified by extending the surface and installing a 3- by 4-inch air jet which exhausted into the air above the table. A schematic diagram of the wave table is shown in figure 1. A blast wave was created by a 13.5-gram, spherical-cast, bare, 50/50 pentolite charge detonated by an instantaneous electric blasting cap supported as shown in reference 9. The height of burst used was 3 inches so as to take advantage of the charge-doubling effect of the reflected wave from the table and to ensure that the triple point was well above the field of flow used. The instruments used to determine the overpressure and time duration over the extended area of the table were the pressure pickups and chronographs described in reference 9.

The two-dimensional wing model was a 9-percent-thick symmetrical airfoil of shape roughly similar to the NACA 0009-64 airfoil. The chord was 0.353 inch and the span was 3 inches. It was supported at the midchord at two spanwise locations (1/4 and 3/4) by two 1/16-inch-diameter drill rods connected to a support system, as shown in figure 2(a). The model leading edge was placed 8 inches above the table, centered spanwise

over the jet, and located 1/4 inch from the center of the jet leeward of the blast along the blast line; it was then a horizontal distance of 11.85 feet from the center of blast.

The air jet was remotely controllable and was set to run continuously during a test at a constant Mach number of 0.1 at the airfoil position above the table. The velocity profile of the air stream at this position above the table was found to be approximately flat in both the spanwise and normal directions with more than 85 percent of the model span within 4 percent of the design velocity (M = 0.1) of the jet at 8 inches above the table, and the ends of the model span in flow of not less than 80 percent of design velocity. These numbers apply to the blast-displaced jet as well as to the initial jet position. It is believed that the model support rods in front of the model had a negligible interference with the blast wave.

The axis of the two-mirror, parabolic, 6-inch-diameter optical system (adjusted for schlieren) (see fig. 2(b)) was parallel to the model span with the light source and knife edge adjusted for on-axis operation. The system was supported from the leeward side and was in no way attached to the table. Light shields were placed around the light path between each mirror and its optical component (that is, knife edge or light source). However, the shields were terminated far enough from the model to ensure against the entrance of wave reflections from the shields into the model flow field during the test time.

The model support system, as shown in figure 2(b), was attached to the model on the blast side so as to allow for unobstructed viewing of the leeward flow field by the optical system. The support arms were airfoil shaped with sharp edges and were alined with the blast flow so as to produce a minimum reflection of the blast wave. The model support system was attached to the schlieren supporting system and did not cross the air jet stream. Most of the data were taken before any visible reflections from this support system entered the field of view, and data subsequent to this time will be so designated. No other reflections could enter the model flow field during the time of these tests, including reflections from the jet exit opening in the table as well as reflections from the schlieren-support beam. Reflections of the blast wave from the free-air jet boundary were considered negligible, inasmuch as the ratio of density of room air to jet air was 0.995.

SCOPE OF TESTS

The free-flight and blast conditions of reference 1 were simulated by placing the model in the steady-flow free air stream and detonating

the high explosive charge at a scaled distance from, and normal to, the model chord. The air-stream velocity and blast-wave peak overpressure were identical to that of reference 1, and the time duration of positive overpressure was 1/20 that of reference 1, so that the model chords of forward flow during the positive duration were also identical. In fact, the Reynolds number of the test was the only aerodynamic parameter not nearly identical to the case simulated, and it is believed that this similarity parameter is probably not significant in the present study. (See ref. 10.)

A set of schlieren photographs was obtained over a range of time delays for the configurations listed in table I and shown in figure 3. The time delays were arranged to include early photographs showing the shock (blast-wave front) somewhere near the model, as well as to include photographs for subsequent times up to the times at which interference waves from the equipment would show in the photographs. The largest amount of data, however, was obtained with configuration 1 (fig. 3(a)), since this model represented simulation of conditions of reference 1 and could be used for comparisons of results. The pertinent test conditions of reference 1 are also shown in table I for ready comparison.

It should be pointed out that the blast-wave flow does not strike the airfoil exactly normal to the chord in configurations 1, 2, and 3, as originally intended. This difference is due to the fact that the model is 8 inches above the surface and the blast wave is hemispherical in shape and would therefore be exactly normal only if the model were at the table surface. For these configurations, the blast-wave flow was found from photographs taken at $t \approx 0$ to strike the model at approximately 86° to the chord, rather than 90°. This fact was overlooked during the test programing and the model was set with respect to the table surface. For configurations 4 and 5, the model support system was rotated and the model likewise set with respect to the table surface. In addition, for configuration 5, the charge was moved to a point 7.6 feet from the model. These slight variations from the proposed test conditions are not believed to be significant in comparisons of the pertinent results with those of reference 1 nor in the comparisons of the results of configuration 1 with configuration 5.

RESULTS AND DISCUSSION

Schlieren Photographs

Schlieren photographs of the series obtained for configuration 1 are shown in figure 4. Schlieren photographs of configurations 2, 3, 4, and 5 are shown in figures 5(a), (b), (c), and (d), respectively. From these

photographs a well-defined vortex is shown to be formed at both the leading edge and trailing edge of the airfoil at about the time of shock diffraction about these points, and the vortices move downstream with time in essentially the direction of the resultant fluid flow. It is also seen, for the cases where the resultant-flow angle of attack is not near 90°, that the leading-edge vortex moves at a speed considerably less than the trailing-edge vortex. After the leading-edge vortex in configuration 1 (fig. 4) has proceeded to a point about 50 percent of the chord, the vortex has become less well-defined and its center is difficult to identify accurately. From this observation, the plots of the movement of the vortex for configuration 1 with any time-dependent parameter will obviously become less accurate as time increases. Inasmuch as each photograph represents a different test, some random scatter of data likely results from lack of exact control of all test conditions. For configurations 3, 4, and 5 (fig. 5), the vortex is noted to be somewhat more well-defined than for configuration 1. Reflections from the support bar are seen to enter the flow field after about 530 microseconds for configurations 1, 2, and 3. Since this bar is farther away in configurations 4 and 5, no reflections are seen for these cases.

Presentation of Results

The results obtained from measurements of the vortex position in the photographs are given in figures 6 to 9. Figure 6(a) shows the ratio of the vortex chordwise displacement to the free-stream fluid chordwise displacement as a function of the free-stream chordwise displacement for the leading-edge vortex. Figure 6(b) shows the results for the normal component in the same manner as used for the chordwise component. Figures 7(a) and 7(b), respectively, show the chordwise and normal components of the trailing-edge vortex results. Figures 8(a), 8(b), 9(a), and 9(b), however, show the actual vortex position with respect to the airfoil as a function of time for the chordwise and normal components of the leading- and trailing-edge vortices, respectively. In figures 6 to 9 the horizontal bars on a few typical points show the range of uncertainty of locating the center of the vortex for configuration 1. For the other configurations the range of uncertainty is much less than this. The flags indicate data after wave reflections have entered the flow field.

It appears to be both logical and convenient to present the fluid flow and vortex movements about the airfoil in terms of only two components, namely, the component in a chordwise direction and the component normal to the chord. Presentation in this form is convenient in the cases of a simulated forward movement with the blast striking from a direction normal to the chord, because the chordwise component of the free stream is that due to flight only, and the changes in free-stream flow due to the blast are seen only in the normal component. Each of

these components of the vortex movements is plotted in terms of the corresponding free-stream flow component in figures 6 and 7. In other words, the vortex is seen to move in a certain manner with regard to the free-stream fluid movement. Use of this concept essentially eliminates the direct consideration of the time-dependent parameters of angle of attack and resultant velocity, and in fact, of time itself. Since the measured parameter is the vortex position (not vortex velocity) the plots are made by using the chordwise and normal components of this parameter in terms of the corresponding component of the free-stream fluid position. Position is then defined as the displacement during time t of the vortex or free-stream fluid, with $t = 0$ being the time at which the vortex was generated.

The displacement of the free-stream fluid during a given time must first be computed. In the case of the component due only to flight, this displacement is obtained simply as a constant velocity times a time. For the free-stream fluid movement due to the blast, however, a special computation is required because of the time-dependent nature of the flow induced by a spherically diverging wave system. This computation involves integration of an analytical approximation for the time dependency of flow velocity in the blast and is given in appendix A.

The free-stream fluid displacements in a chordwise and normal direction, respectively, are then found for all the configurations from the following equations:

$$x_R = u_0 \cos \alpha_0 t + l \cos \alpha_B \tag{1}$$

$$y_R = u_0 \sin \alpha_0 t + l \sin \alpha_B \tag{2}$$

The value of $l = f(t)$ is found in figure 10 as computed in appendix A, and the other parameters are found in table I.

Discussion of Results

The first obvious comparison to be made is that of the leading-edge vortex chordwise displacement of configuration 1 with the load-peak displacement of reference 1. It is seen in figures 6(a) and 8(a) that the movement of the vortex is closely similar to the load peak travel of reference 1, but that the load peak is consistently slightly forward of the vortex center even when allowance is made for scatter of the data. There is no apparent explanation of this result in terms of model dissimilarity, since the sharp-leading-edge data of configuration 2 show

no significant difference from the rounded-leading-edge data. This latter result also suggests that there would be small or no effect of scale, as was previously suggested. No theoretical treatment of the vortex problem which exists for this condition is known, but it may be that the difference between load-peak and vortex location is actually plausible. In any case, it appears that the problem might be clarified somewhat if the actual pressure distribution along the upper and lower surfaces were obtained in flight or tunnel tests.

Figure 6(a) clearly shows that the leading-edge-vortex chordwise displacement for all the configurations shown is approximately a constant value of one-third of the free-stream fluid chordwise displacement. That is, this vortex chordwise movement is at a velocity of one-third the free-stream velocity. (It should be noted that plots such as figures 6 and 7 are indicative of changes of relative velocity which occur but do not indicate velocity magnitude other than for the special case of vortex and free-stream fluid velocity constant in time.) Again, no known theoretical treatment is available for such a vortex problem from which a number such as one-third may be derived. Intuitively, however, the velocity should be expected to be of the order of one-half of the free-stream velocity, since the vortex is exposed to the stream on the one side and to a separated region on the other. In figure 7(a) the chordwise displacement of the trailing-edge vortex appears to be more nearly that of the free-stream fluid for the configurations shown, although it appears to start out more slowly and then to accelerate in the chordwise direction. Also, for configurations 1 and 2, the vortex starts out more slowly than for configurations 4 and 5 in a chordwise direction, and this result is probably due to the existence of a well-developed wake for the cases of initial steady-flow field about the airfoil. The fact that it starts slowly in configurations 4 and 5 is possibly due to some velocity defect in the field close behind the airfoil even this early in the flow development time. In either case, the vortex is not initially exposed to the full free-stream component of the flow.

With regard to the normal components of the vortex and stream movements it is seen in figure 6(b) that for all the configurations the leading-edge vortex displacement is in the range of one-fourth to one-half that of the free stream. In this case, as in the case of the chordwise component, the leading-edge vortex is not fully exposed to the free-stream normal-flow component, since it is on the sheltered side of the airfoil with regard to the blast-wave flow. For example, the data of configurations 1 and 2 show a relative slowing up of the vortex, and the vortex is moving along the upper surface of the airfoil and is more shielded from the free-stream normal-flow component. For configuration 3, the vortex is located much farther above the upper surface and is not moving chordwise and probably for this reason of greater exposure shows greater relative displacement. For configuration 5, the vortex is less shielded

from the blast component than for configuration 1, simply because the flow is actually induced from the 31° direction by the blast wave, whereas, for configurations 1 and 3, this component is separately induced from the 86° direction.

In the case of the normal component of the trailing-edge vortex, figure 7(b) shows that the displacements for virtually all configurations start out between 0.8 and 1.0 of the free-stream fluid. It appears that in the case of configuration 3 the vortex is slowing somewhat in the normal direction and this result may be due to the fact that the vortex is not exposed fully to the free-stream fluid component, since for this case the vortex is not swept rearward away from the airfoil to such an exposed degree.

An interesting point to note from the data shown in figure 6(a) is the lack of any influence due to blast-wave angle of attack on the chordwise component of the vortex relative movement. This result implies (as one might expect) that the formation of the vortex is dependent on the resultant fluid flow and not on the manner in which this flow is produced.

Examination of the results plotted as shown in figures 8 and 9 brings out more clearly the dependency of the vortex movement on that of the surrounding fluid. The data for configurations 1 and 2 exhibit a different timewise dependency than that of configurations 4 and 5 when the chordwise components (figs. 8(a) and 9(a)) are considered. The timewise dependency of the free-stream resultant flow (similar to the chordwise component) is shown in figure 11 for configurations 1 (or 2) and 5 (or 4). A distinct difference is found in the character of the timewise dependency of the flow. On the other hand, the normal components (figs. 8(b) and 9(b)) show close similarity, since the timewise dependency of this component of the free-stream flow is also quite similar. These timewise differences will be reflected in the loadings, inasmuch as the loading changes on the airfoil have been shown to be associated with the vortex chordwise movements in reference 1. These timewise loading differences would also be found between results from flight and shock-tube studies, since a similar (as between configurations 1 and 5) comparison of the timewise flow character (see fig. 11) would also apply.

It is interesting to compare the vortex movements of configurations 3, 4, and 5 with that predicted by Rott (found in ref. 6) for the vortex produced in a shock tube at the leading edge of a wedge. Rott's theory is interpreted in terms of the free-stream fluid flow and airfoil shape in such manner that, by the use of an equivalent free-stream velocity, along with an equivalent wedge angle, the timewise variation of the free-stream flow and nose roundness is essentially eliminated. The results of such a comparison are shown in figure 12. The equivalent velocity was determined as

$$u_e(t) = \frac{l}{t} \tag{3}$$

where l is found in figure 10, and the equivalent wedge angles used were 30° and 14° for the leading and trailing edges of the airfoil, respectively. For convenience, Rott's equation is reproduced as follows:

$$\frac{r}{a_2 t} = 2\left[\frac{nM_2 \sin n\pi \sin n\alpha \cos n\left(\beta - \frac{\epsilon}{2}\right)}{2\pi}\right]^{\frac{1}{2-n}} \tag{4}$$

Although the application of Rott's theory to this flow may be thought of as rather crude, it is seen that the vortex movement is described quite closely for configurations 4 and 5, with not so good agreement for configuration 3. As a further comparison, the initial blast-wave flow velocity u_2 was used in place of an equivalent velocity u_e and it is seen that the agreement is in all cases poorer. This result appears to be a further indication of the dependency of the vortex movement on that of the surrounding fluid.

CONCLUDING REMARKS

Measurements have been made of the vortex movements with time of both the leading-edge and trailing-edge vortices formed about an airfoil in simulated subsonic flight undergoing a blast of sufficient strength to exceed momentarily the stall angle.

These measurements, along with those obtained for the case of no-flight simulation but blast of such strength and orientation to produce the same maximum resultant angle of attack and velocity result in the following conclusions:

1. The chordwise movement of the leading-edge vortex is closely similar to the chordwise load-peak movement of a free-flight model twenty times as large under similar conditions. It may be that the load peak is slightly forward of the vortex center.

2. No detectable differences in the vortex movements were noted when the airfoil was reversed so as to provide a sharp leading edge and a rounded trailing edge. This result also suggests that there is little or no effect of scale for these conditions.

3. The vortex movement is evidently dependent primarily, if not entirely, on the movement of the fluid about the vortex.

4. No effect of blast-wave orientation on the vortex movements relative to the fluid was noted.

5. For the cases where the vortex is surrounded largely by the free stream (trailing-edge vortex), the vortex movement is generally at the free-stream velocity.

6. For cases where the vortex is only partially exposed to the free stream or is exposed to separated regions (leading-edge vortex), the vortex movement is on the order of one-third to one-half of the free-stream velocity.

7. It is shown that cases which exhibit a different timewise dependency of the fluid movement with respect to a body likewise exhibit a different timewise dependency of the vortex movement or loading with respect to the body.

8. Comparison of the vortex movements for the no-flight simulation cases with a theory by Rott developed for shock-tube flow about a wedge yields good agreement when an alteration of the theory is made so as to apply to the quasi-steady conditions.

Langley Aeronautical Laboratory,
National Advisory Committee for Aeronautics,
Langley Field, Va., October 11, 1957.

APPENDIX A

COMPUTATION OF BLAST FLUID FLOW

Consider the case of a spherical blast wave in which it is assumed the variation of overpressure with time may be represented by the following expression up to values of $t'/t_d = 2$; this expression has been suggested in a number of places in the literature (for example, see ref. 11), and was found to fit closely the pressure-time curves available:

$$\frac{p - p_0}{p_2 - p_0} = \frac{1 - \frac{t'}{t_d}}{e^{b\frac{t'}{t_d}}} \tag{A1}$$

where b is a constant for a given blast-wave-peak overpressure $p_2 - p_0$. Let it be assumed further that the value of b may be found by evaluating equation (A1) at $\frac{t'}{t_d} = 2$ by using values of the peak negative overpressure from reference 12. If it is assumed that, in the region behind the spherical shock wave $\left(0 < \frac{t'}{t_d} < 1.0\right)$, the fluid entropy is constant (a reasonable assumption for the weaker shock cases, $\frac{p_2}{p_0} < 2.0$), then the relation between fluid velocity and overpressure is found from Riemann's isentropic unsteady flow relations, which yields for air (when $\gamma = 1.40$):

$$\frac{u}{u_2} = 1 + \frac{5}{M_2}\left[\left(\frac{p}{p_2}\right)^{1/7} - 1\right] \tag{A2}$$

The value of M_2 is found as a function of $\frac{p_2}{p_0}$ from the Rankine-Hugoniot shock relations applied to this case.

It can be shown by numerical substitution that equations (A1) and (A2) are very closely satisfied over a range of blast-wave overpressures, $0 < p_2 - p_0 < 20$ psi, by the following relation,

$$\frac{u}{u_2} = \frac{1 - \frac{t'}{t_d}}{e^{\frac{1}{2}\frac{t'}{t_d}}} \tag{A3}$$

This equation then represents an approximation of the variation of fluid velocity at any fixed reference point, with the time being measured from the time of shock passage at this same point. In order more readily to find the position with time of a particular particle of fluid, the time is now referenced to that of shock passage at a specified fixed point and certain simplifications are made. (See sketch.)

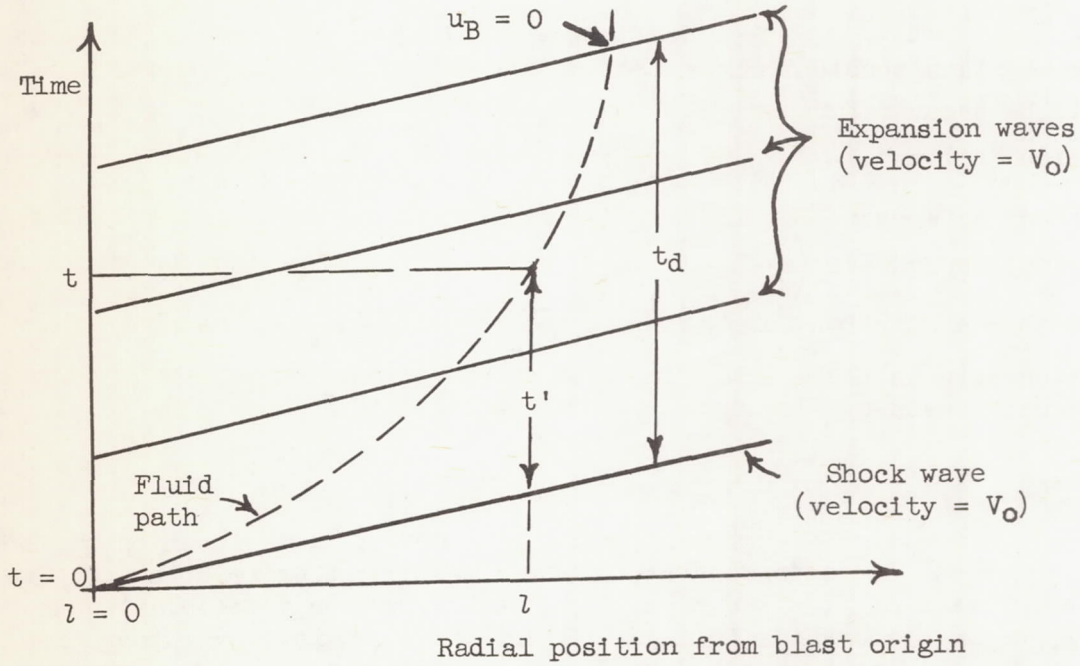

It is here assumed that over a short increment of the total blast travel, the shock travel may be assumed to be at a constant speed. Likewise, the expansion waves, following the shock, are assumed to travel at the same constant speed. Restated, the assumption is simply one of constant shock strength and positive time duration over this increment of space and should be a good assumption for the weaker shock cases and small increments of space. With this model, the following relations are written for the path of a fluid particle starting from $l = 0$ at time $t = 0$:

The fluid velocity at t is

$$u = \frac{dl}{dt} \tag{A4}$$

The fluid time to reach l is

$$t = t' + \frac{l}{V_0} \tag{A5}$$

The variation of fluid velocity with blast time t' at l is already given by equation (A3).

The flow distance l is given by integration of equation (A4) as,

$$l = \int dl = \int_0^t u(t)\,dt$$

and is accomplished by first substituting for dt by differentiating (A5) and inserting $u(t')$ from (A3) and solving for dl to give (A4) in nondimensional form.

$$\frac{dl}{V_0 t_d} = \frac{1}{\dfrac{V_0}{u_2}\dfrac{e^{\frac{1}{2}\frac{t'}{t_d}}}{1-\frac{t'}{t_d}} - 1}\, d\left(\frac{t'}{t_d}\right) \tag{A6}$$

Equation (A6) is then integrated to give l as a function of t' and equation (A5) then substituted into the resulting relation to give l as a function of t. The resulting fluid paths for a few blast-wave overpressures are shown in figure 10 and were obtained by integration of equation (A6), by the method of finite differences.

REFERENCES

1. Pierce, Harold B., and Reisert, Thomas D.: Initial Experimental Investigation of the Aerodynamic Load on the Wing of a Model Caused by a Blast-Induced Gust that Increases the Angle of Attack Into the Stall Region. NACA RM L55H22b, 1955.

2. Reutenik, J. Ray, and Witmer, Emmett A.: Transient Aerodynamics of Two-Dimensional Airfoils. Pt. I - Interferometric Measurements of Two-Dimensional Airflow Development About a Symmetrical Double-Wedge Airfoil in Shock-Initiated Subsonic Flow. WADC Tech. Rep. 54-368 Pt. 1, ASTIA Doc. No. AD-97322 (Contract No. AF33(038)-8906), Wright Air Dev. Center, Aug. 1956.

3. Bleakney, Walker, White, D. R., and Griffith, W. C.: Measurements of Diffraction of Shock Waves and Resulting Loading of Structures. Jour. Appl. Mech., vol. 17, no. 4, Dec. 1950, pp. 439-445.

4. Bleakney, Walker: The Diffraction of Shock Waves Around Obstacles and the Transient Loading of Structures. Tech. Rep. II-3 (Contract N6ori-105), Princeton Univ., Dept. Phys., Mar. 16, 1950.

5. Uhlenbeck, George: Diffraction of Shock Waves Around Various Obstacles Rep. No. 50-1 (Contract No. N6-ONR-232), Univ. of Michigan, Eng. Res. Inst., Mar. 21, 1950.

6. Howard, L. N., and Matthews, D. L.: On the Vortices Produced in Shock Diffraction. Tech. Rep. II-21 (Contract N6ori-105), Princeton Univ., Dept. Phys., July 1955.

7. Geiger, F. W., and Mautz, C. W. (with addendum by R. N. Hollyer, Jr.): The Shock Tube as an Instrument for the Investigation of Transonic and Supersonic Flow Patterns. Project M-720-4 (Contract No. N6-ONR-232), Univ. of Michigan, Eng. Res. Inst., June 1949.

8. Griffith, Wayland: Shock-Tube Studies of Transonic Flow Over Wedge Profiles. Jour. Aero. Sci., vol. 19, no. 4, Apr. 1952, pp. 249-257, 264.

9. Huber, Paul W., and McFarland, Donald R.: Effect of Surface Roughness on Characteristics of Spherical Shock Waves. NACA RM L55B04, 1955.

10. Griffith, W. C., Weimer, D. K., Brickl, D. E., and Bleakney, W.: The Effect of Reynolds Number on the Diffraction of a Shock Wave. Tech. Rep. II-8 (Contract N6ori-105 Task II), Princeton Univ., Dept. Phys., Feb. 1951.

11. Armendt, B. F., Smith, R., and Wise, R. C.: The Initial Decay of Pressure Behind a Shock Front: Comparison of Experimental and Calculated Results. Memo. Rep. No. 997, Ballistic Res. Labs., Aberdeen Proving Ground, Apr. 1956.

12. Curtis, Wesley: Free Air Blast Measurements on Spherical Pentolite. Memo. Rep. No. 544, Ballistic Res. Lab., Aberdeen Proving Ground, July 1951.

TABLE I.- TEST CONDITIONS

Configuration	Model-chord orientation		Blast wave			Jet	Resultant flow	
	With blast flow α_B, deg	With jet flow α_o, deg	Peak overpressure $p_2 - p_o$, lb/sq in.	Positive time duration t_d, microsec	Peak flow velocity u_2, ft/sec	Flow velocity u_o, ft/sec	Maximum angle of attack $\alpha_{R,2}$, deg	Maximum flow velocity $u_{R,2}$, ft/sec
1	86 (fig. 3(a))	0	1.3	1,200	69	113	30	137
2	86 (fig. 3(b))	0	1.3	1,200	69	113	30	137
3	86 (fig. 3(c))	-	1.3	1,200	69	0	86	69
4	31 (fig. 3(d))	-	1.3	1,200	69	0	31	69
5	31 (fig. 3(d))	-	2.65	1,040	136	0	31	136
Ref. 1	90	0	1.4	25,500	75	112	34	136

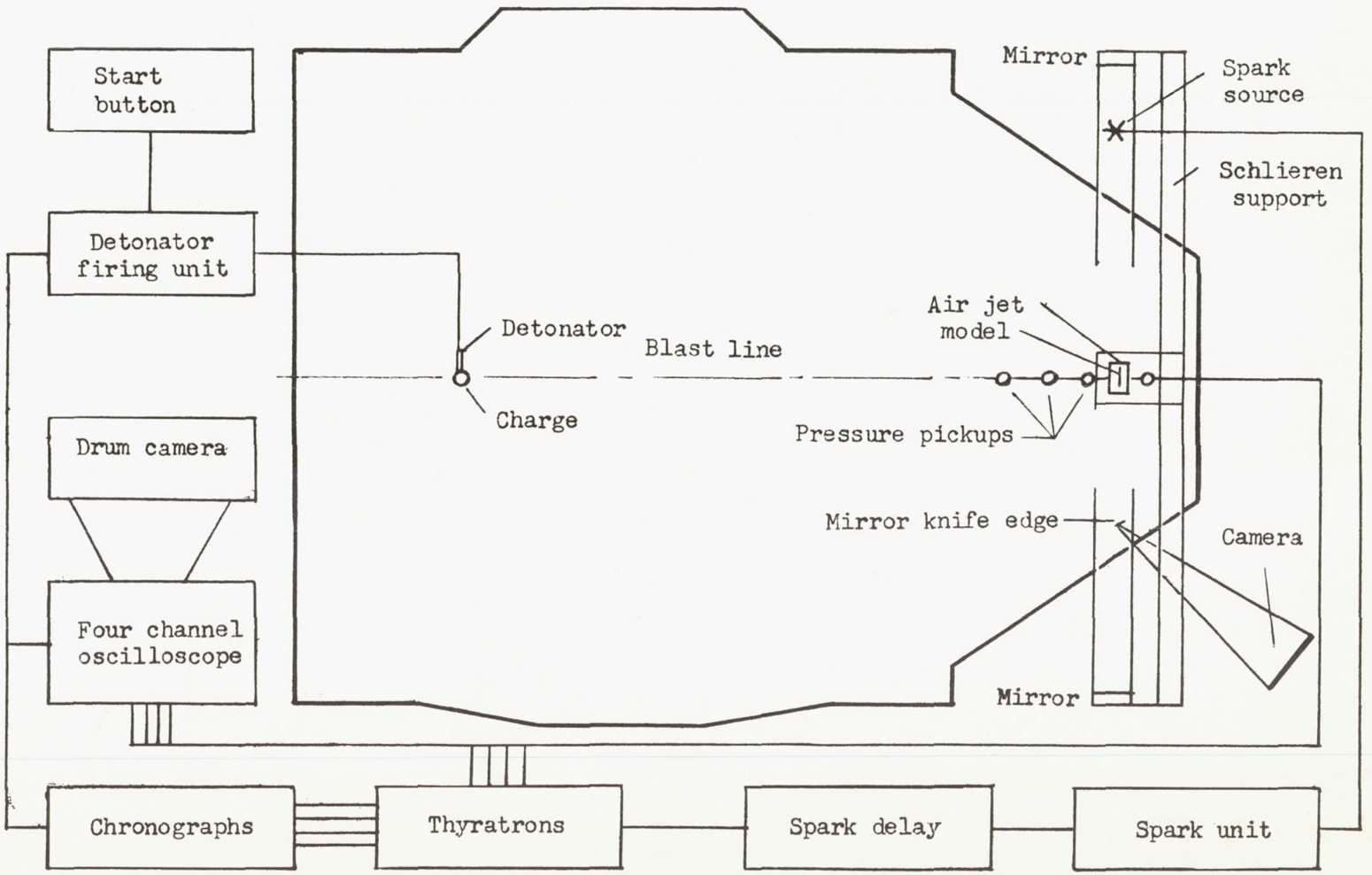

Figure 1.- Schematic diagram of wave table and instrumentation.

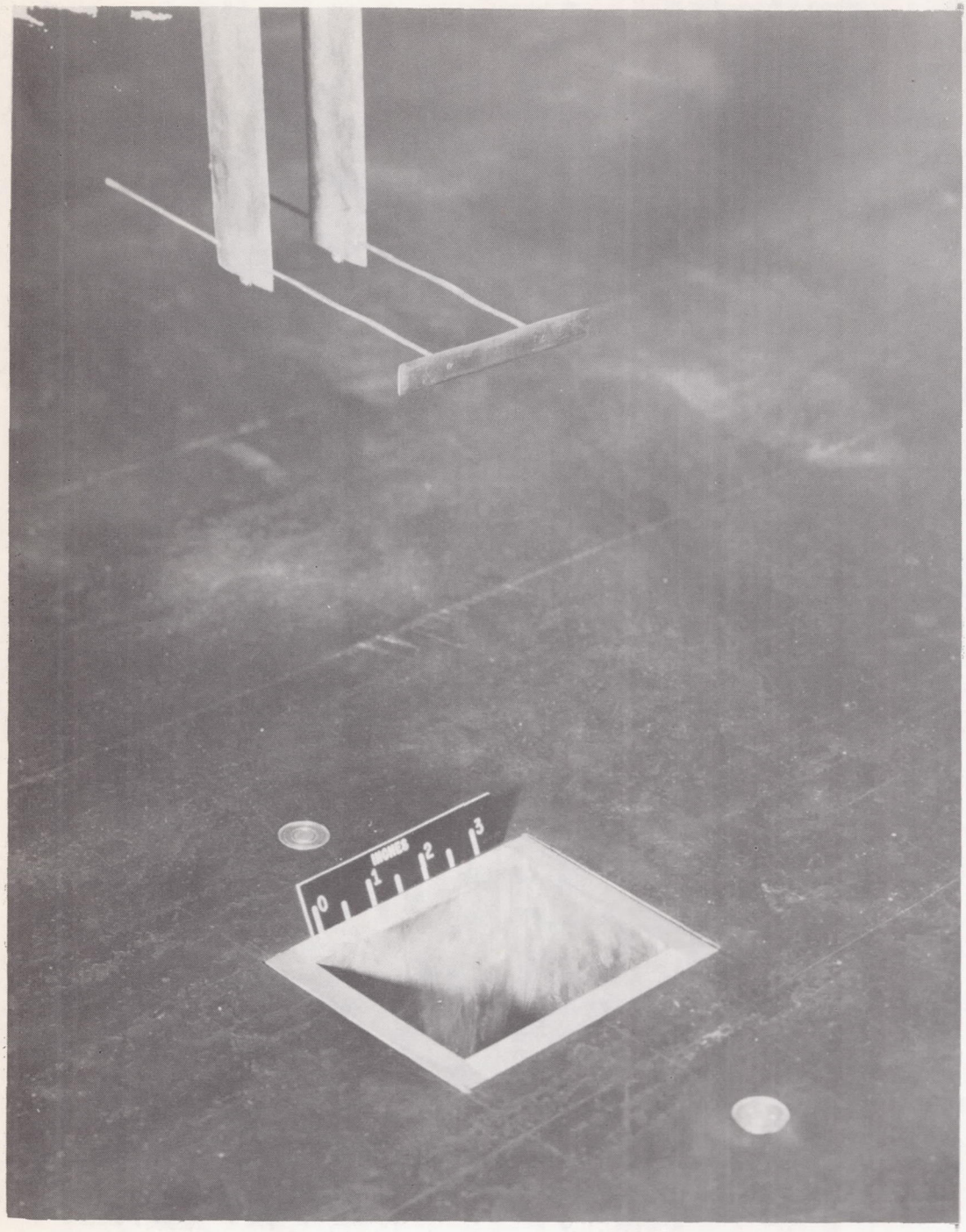

(a) Closeup of model and jet opening. L-57-401

Figure 2.- Model and wave-table arrangement.

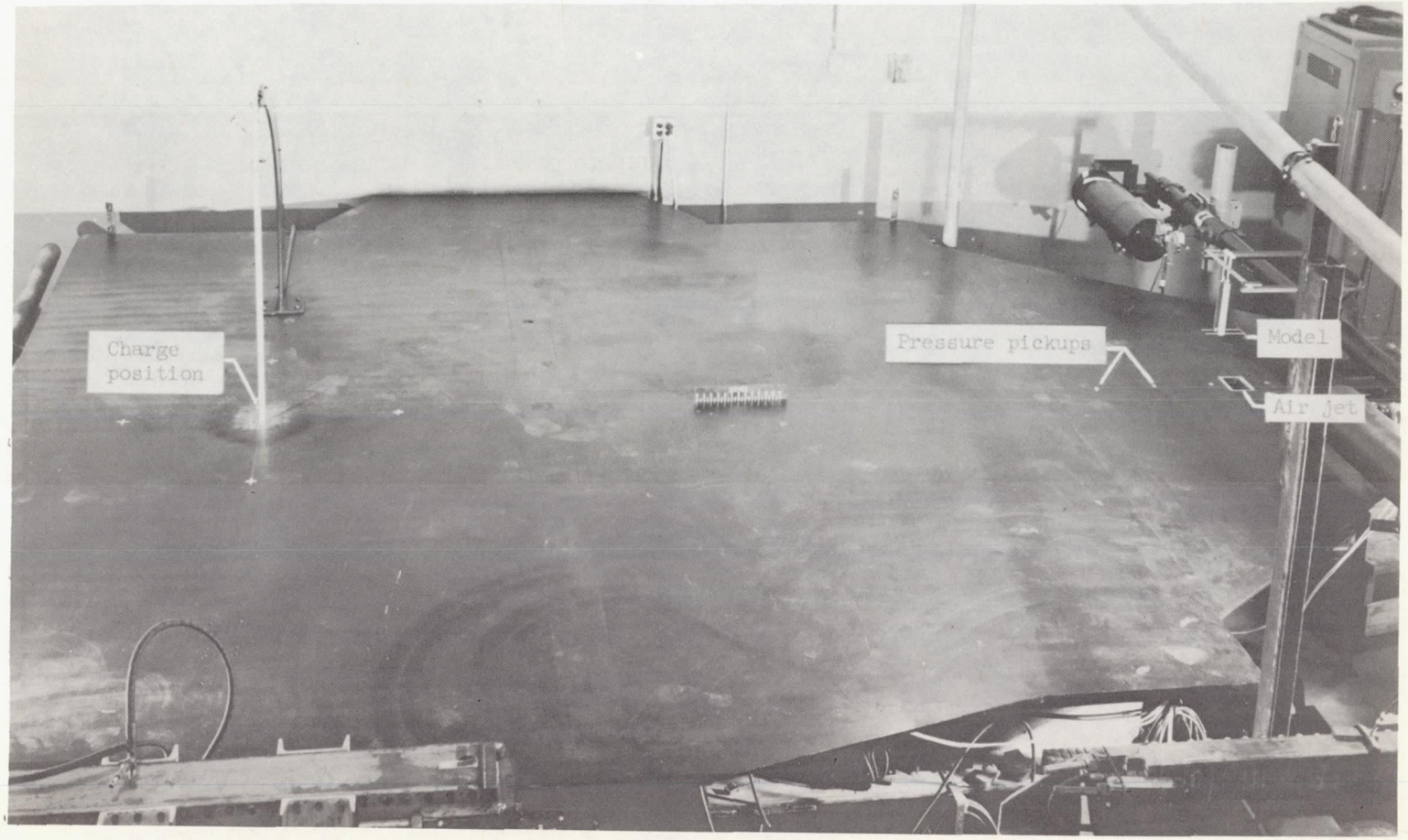

(b) Overall view of wave table. L-57-400.1

Figure 2.- Concluded.

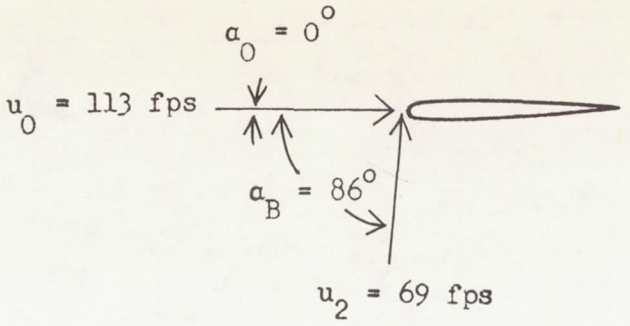

(a) Configuration 1 - round leading edge; jet flow.

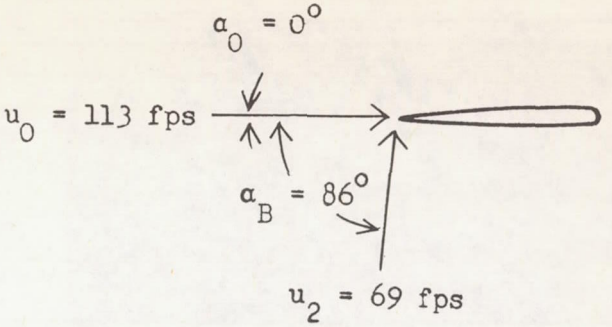

(b) Configuration 2 - sharp leading edge; jet flow.

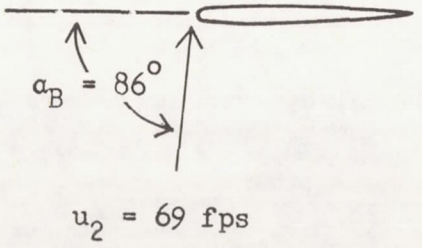

(c) Configuration 3 - round leading edge; no jet flow.

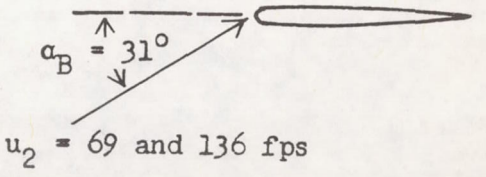

(d) Configurations 4 and 5 - round leading edge; no jet flow.

Figure 3.- Orientation of model with blast wave and jet flow.

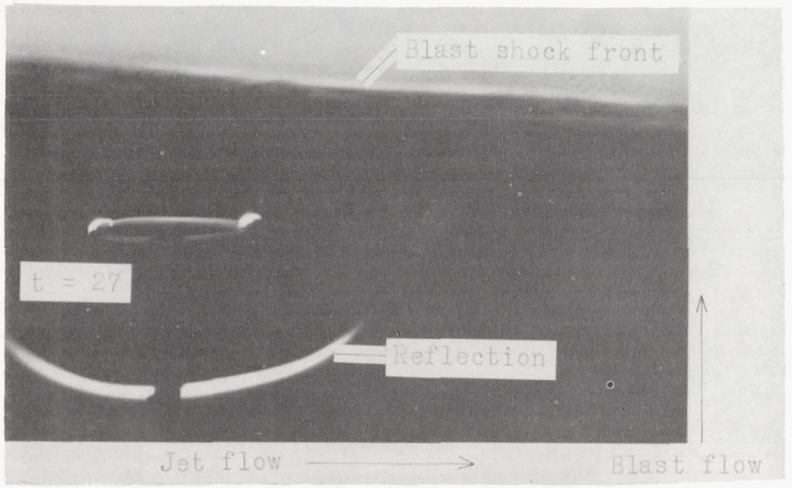

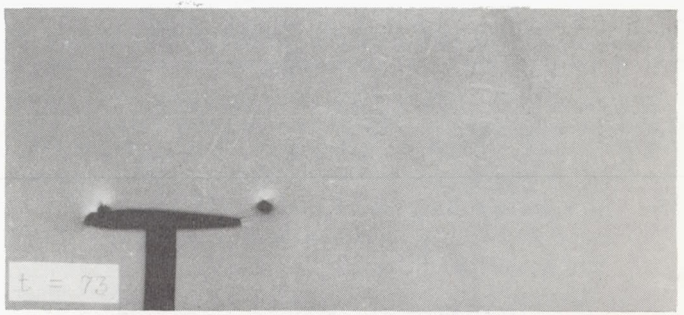

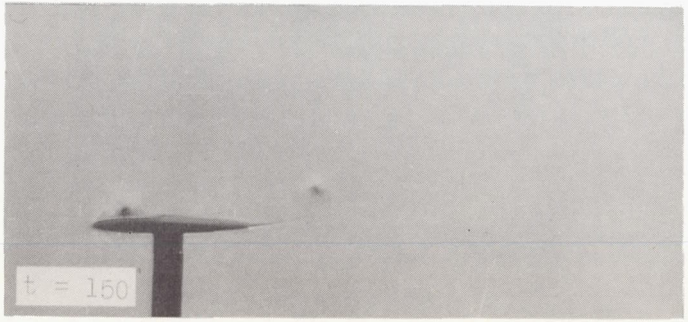

L-57-2785

Figure 4.- Schlieren photographs of configuration 1; $\alpha_B = 86^\circ$; jet flow. Time t is given in microseconds.

Figure 4.- Continued. L-57-2786

Figure 4.- Continued. L-57-2787

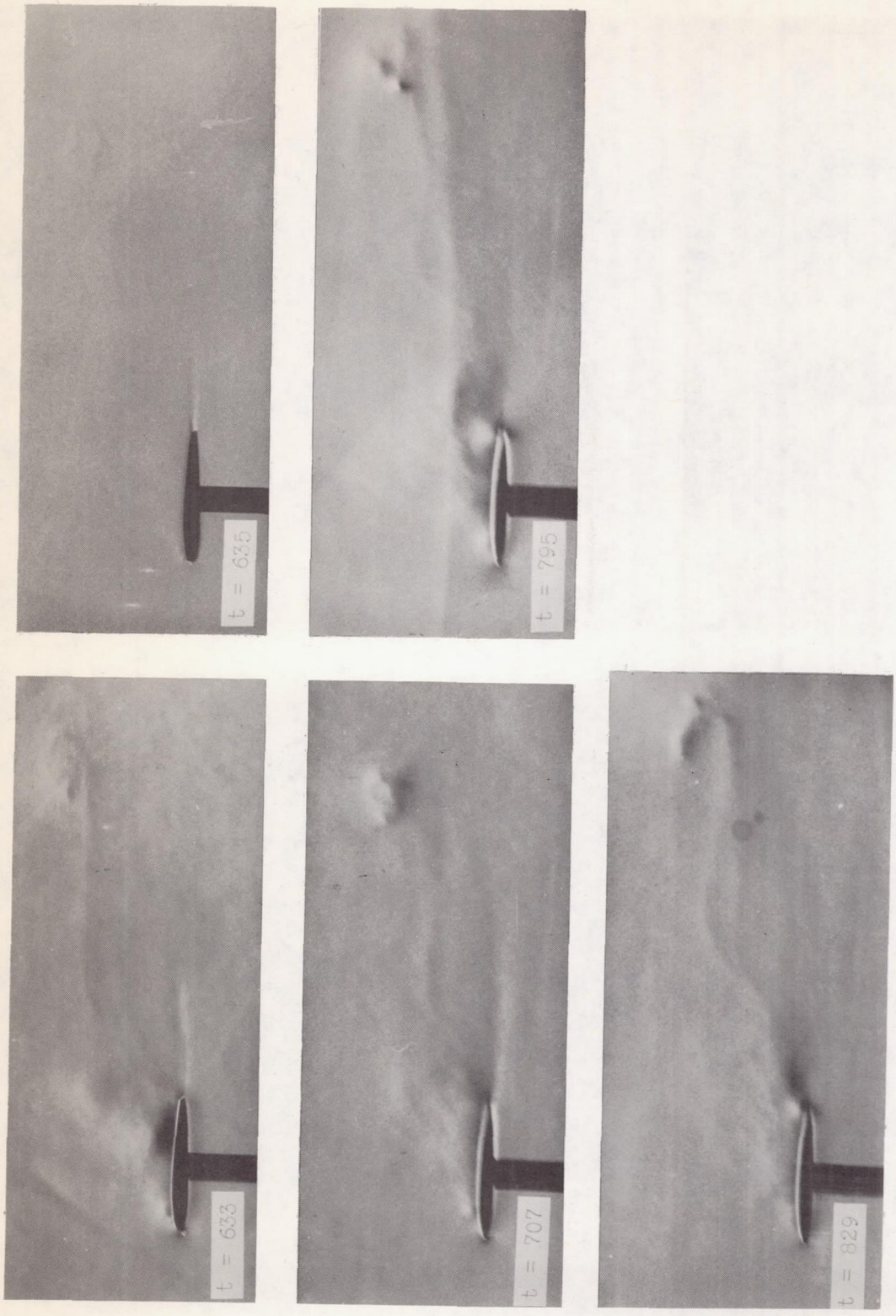

Figure 4.- Concluded. L-57-2788

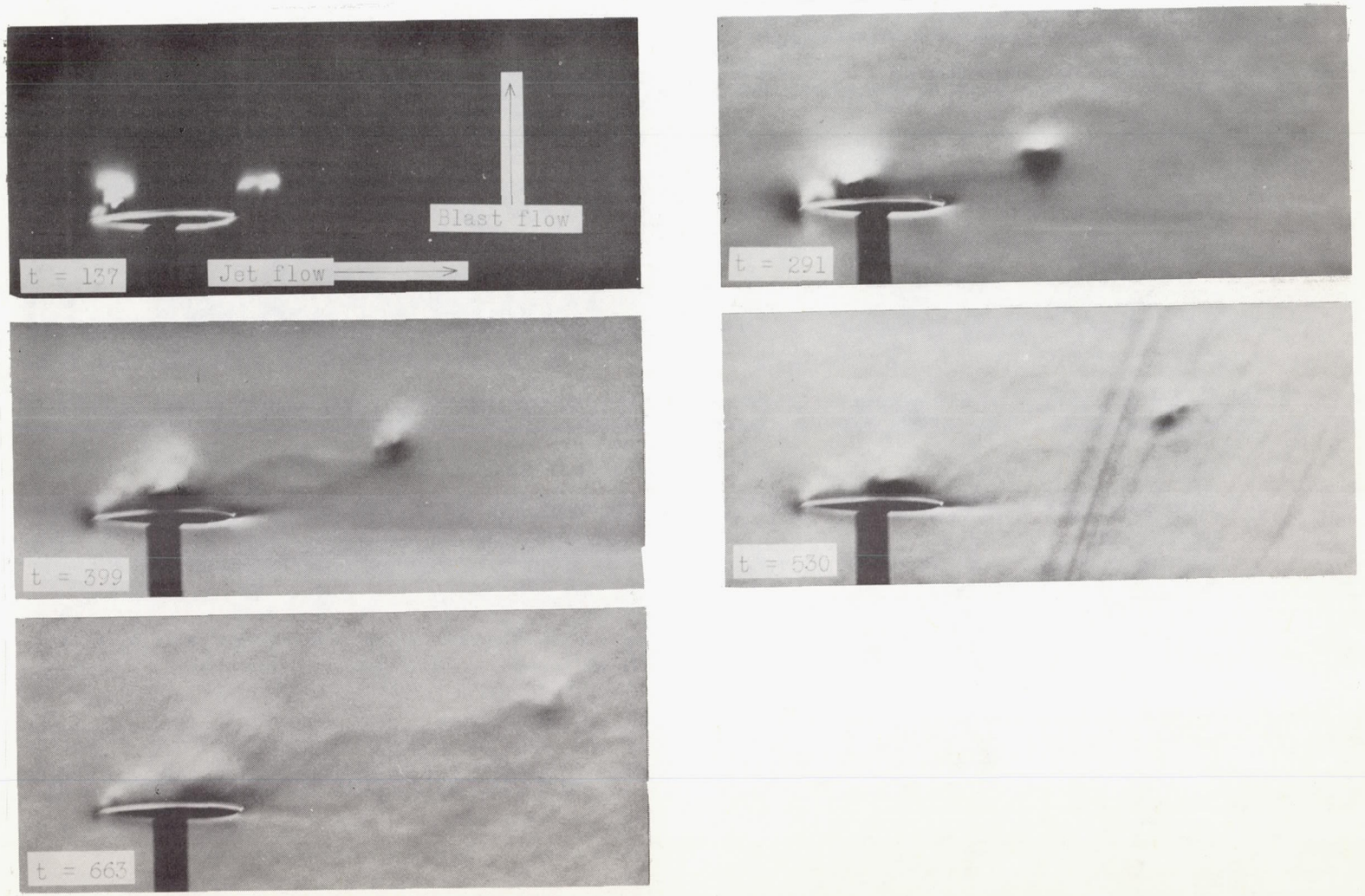

(a) Configuration 2; $\alpha_B = 86^\circ$; jet flow; model reversed. L-57-2789

Figure 5.- Schlieren photographs of configurations 2, 3, 4, and 5. Time t is given in microseconds.

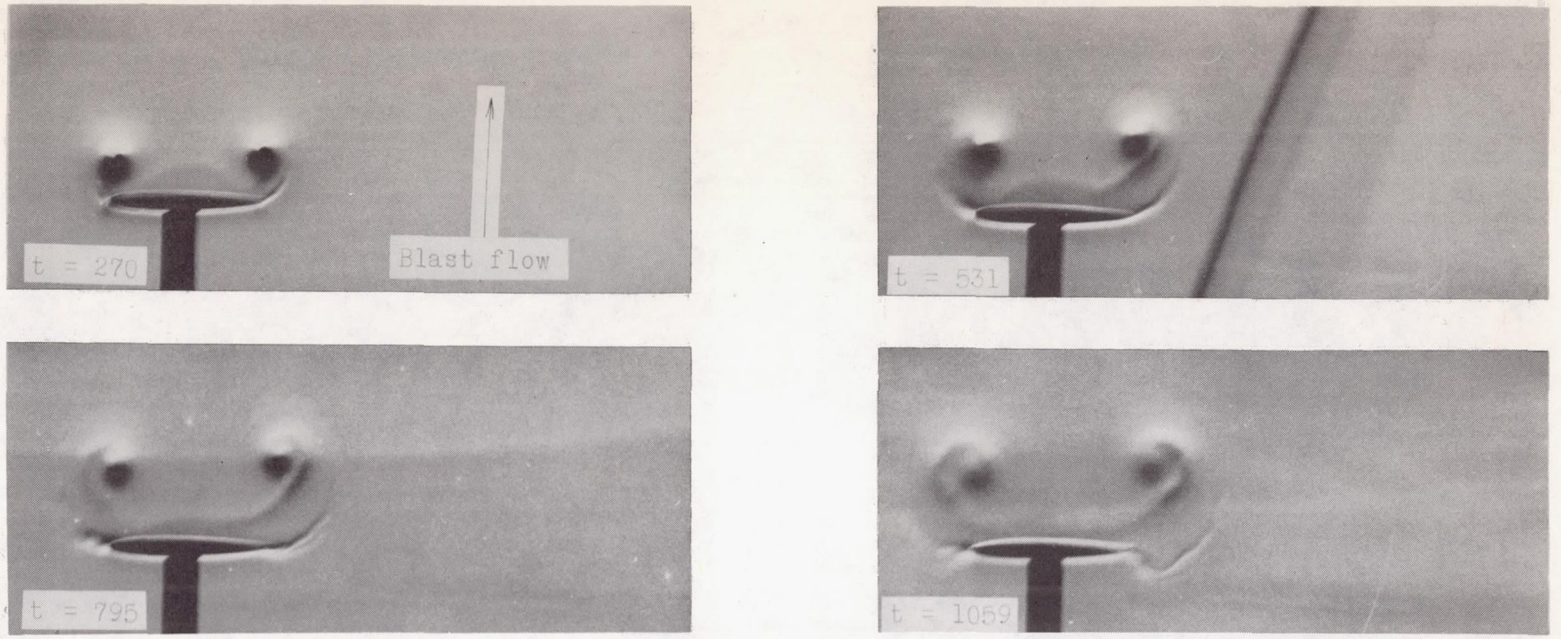

(b) Configuration 3; $\alpha_B = 86^\circ$; no jet flow.

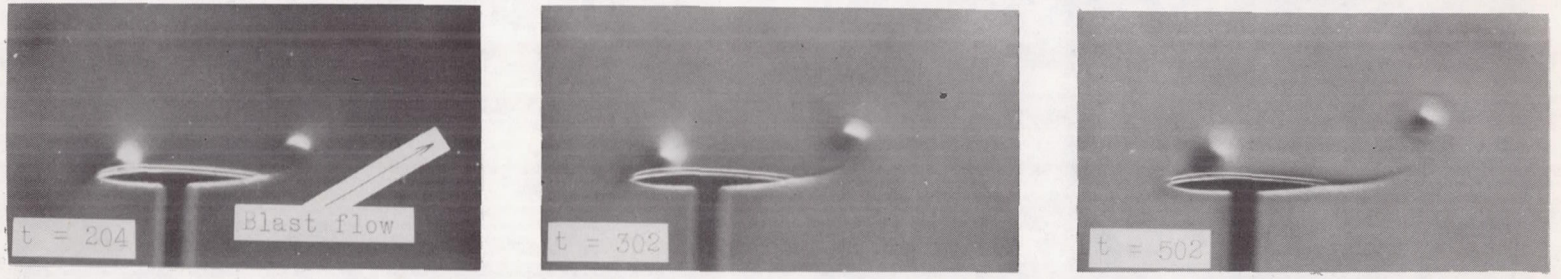

L-57-2790

(c) Configuration 4; $\alpha_B = 31^\circ$; no jet flow; $p_2 - p_0 = 1.3$ psi.

Figure 5.- Continued.

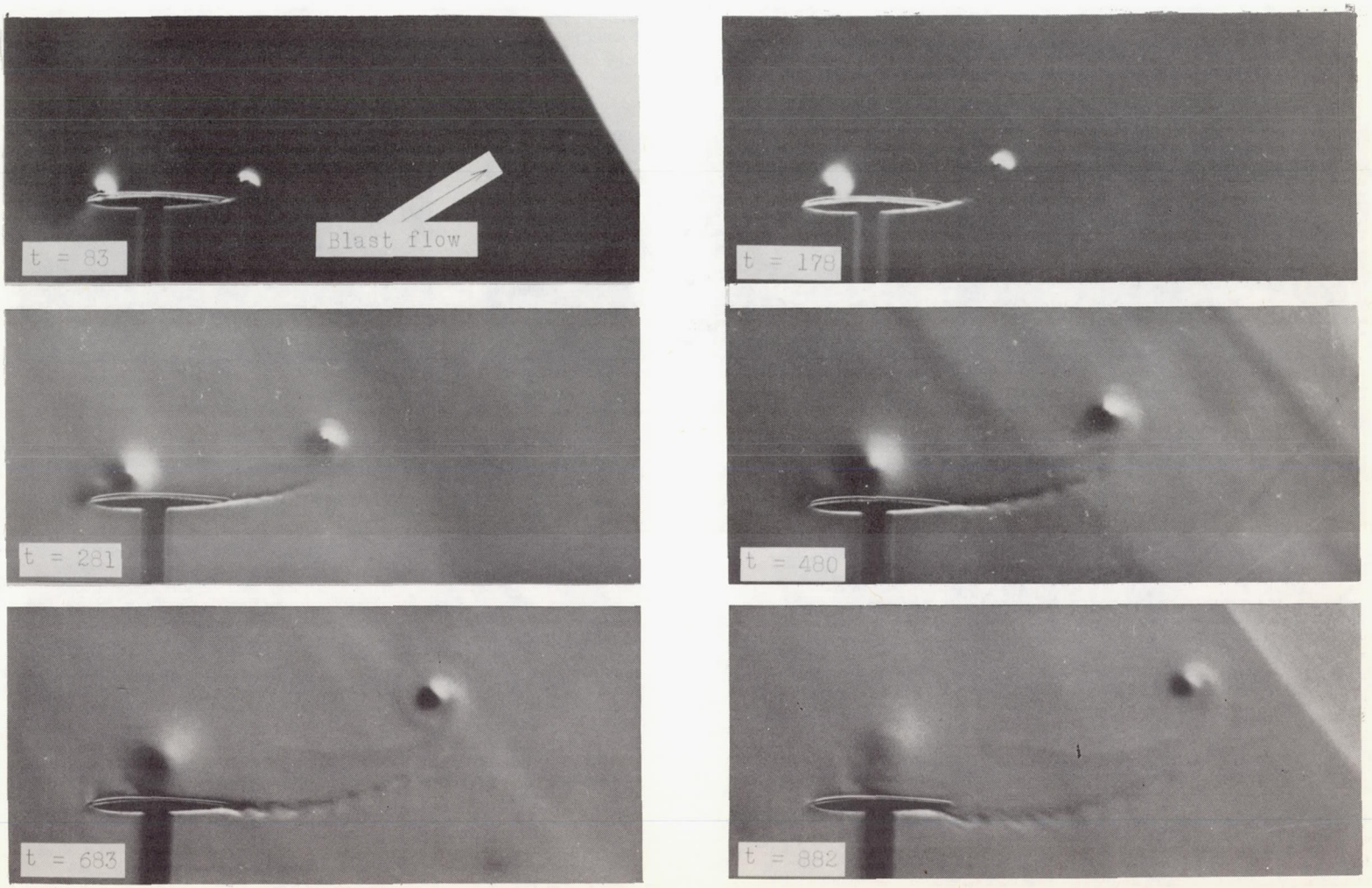

L-57-2791

(d) Configuration 5; $\alpha_B = 31^\circ$; no jet flow; $p_2 - p_0 = 2.65$ psi.

Figure 5.- Concluded.

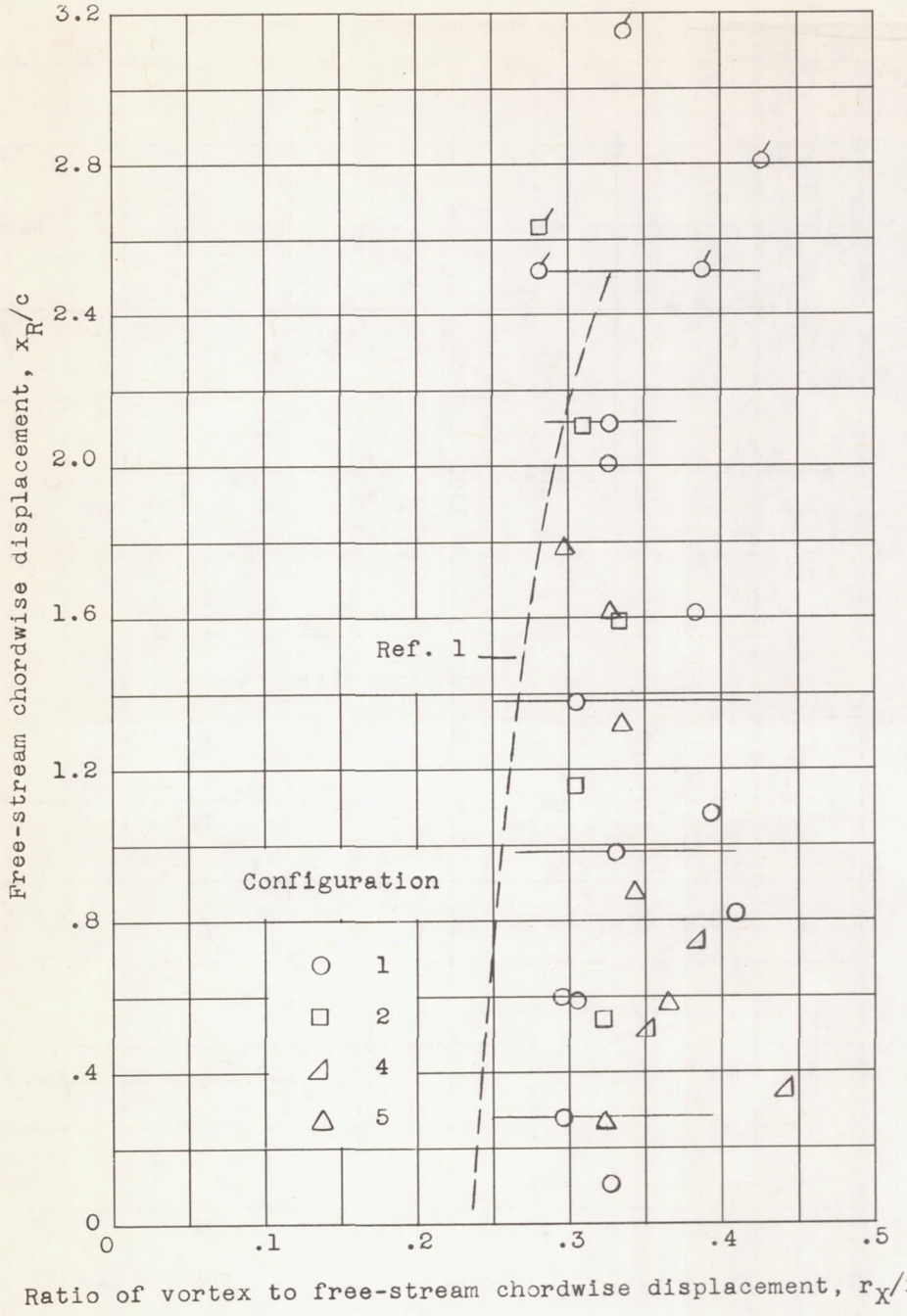

(a) Chordwise components.

Figure 6.- Ratio of leading-edge vortex displacement to free-stream fluid displacement as a function of free-stream displacement. Flags indicate data after wave reflections.

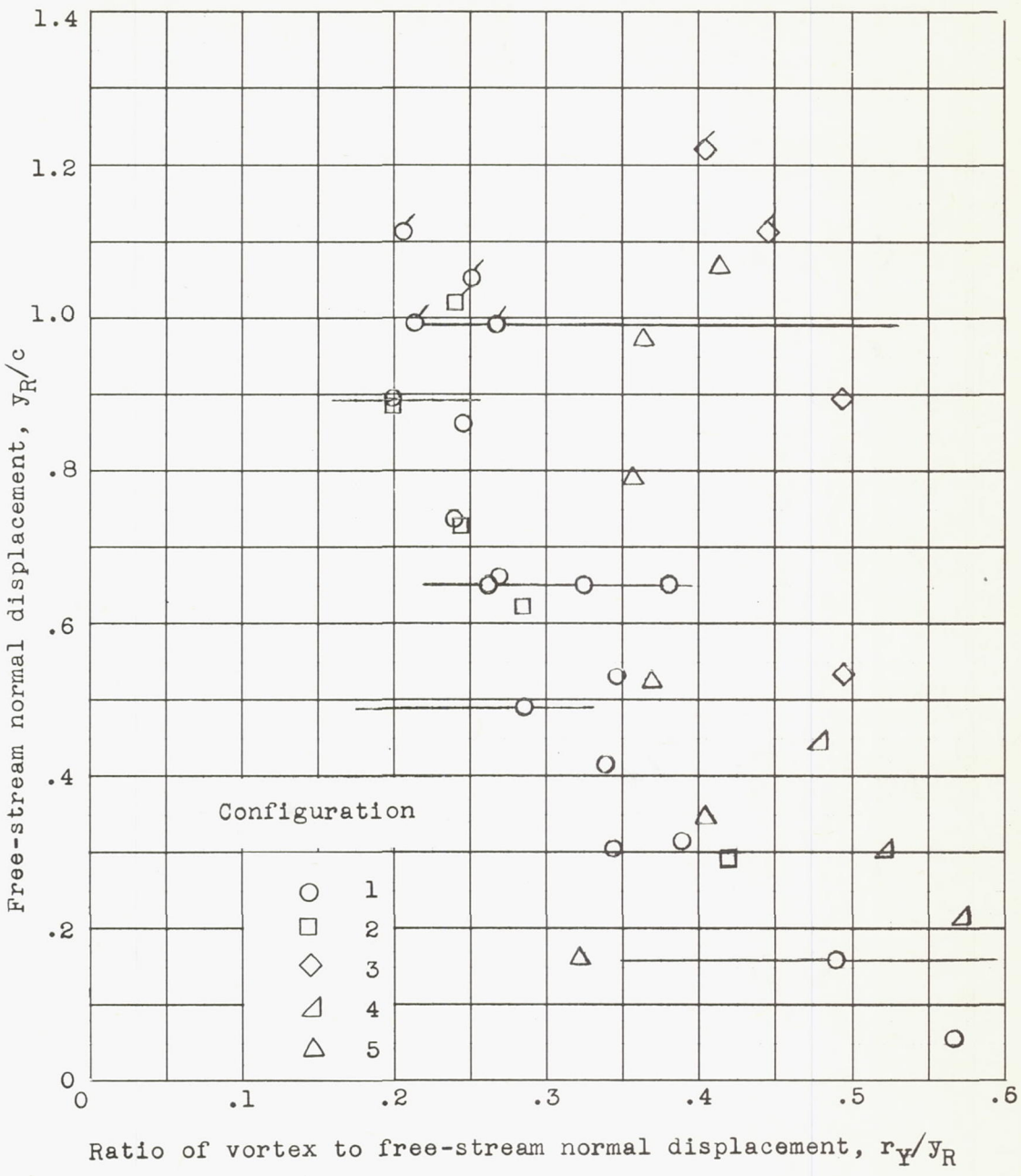

(b) Normal components.

Figure 6.- Concluded.

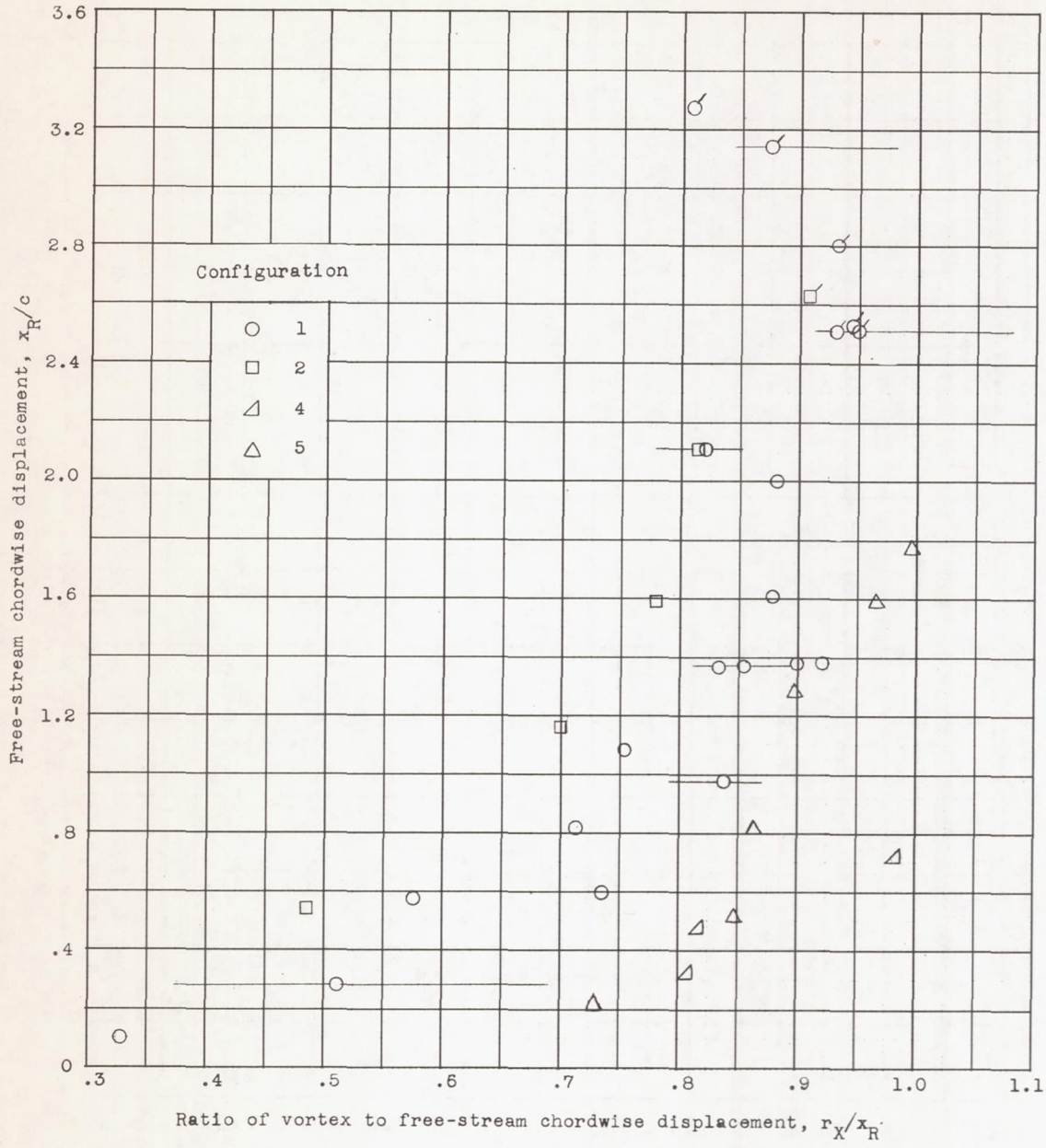

(a) Chordwise components.

Figure 7.- Ratio of trailing-edge vortex displacement to free-stream fluid displacement as a function of free-stream displacement. Flags indicate data taken after wave reflections.

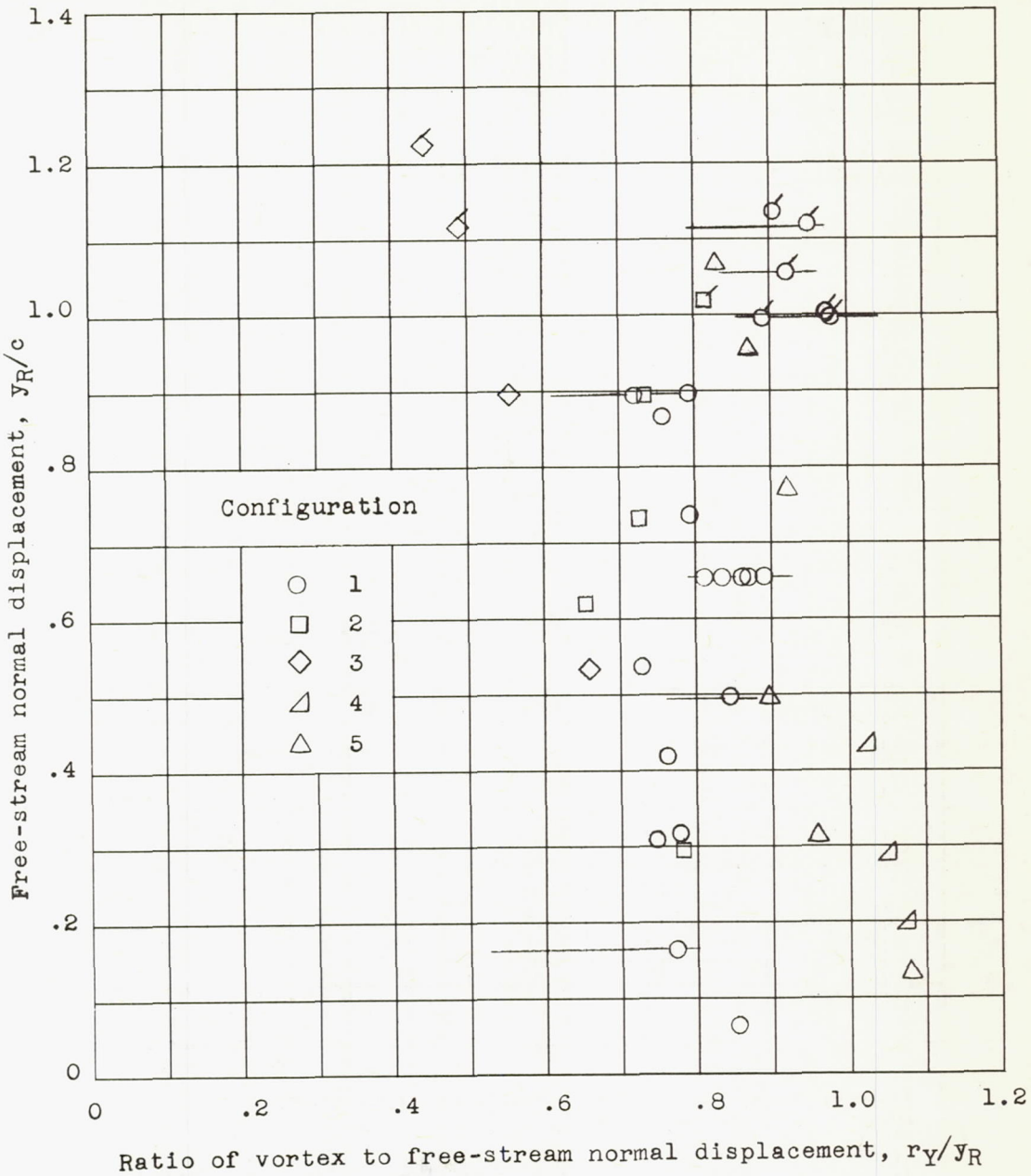

(b) Normal components.

Figure 7.- Concluded.

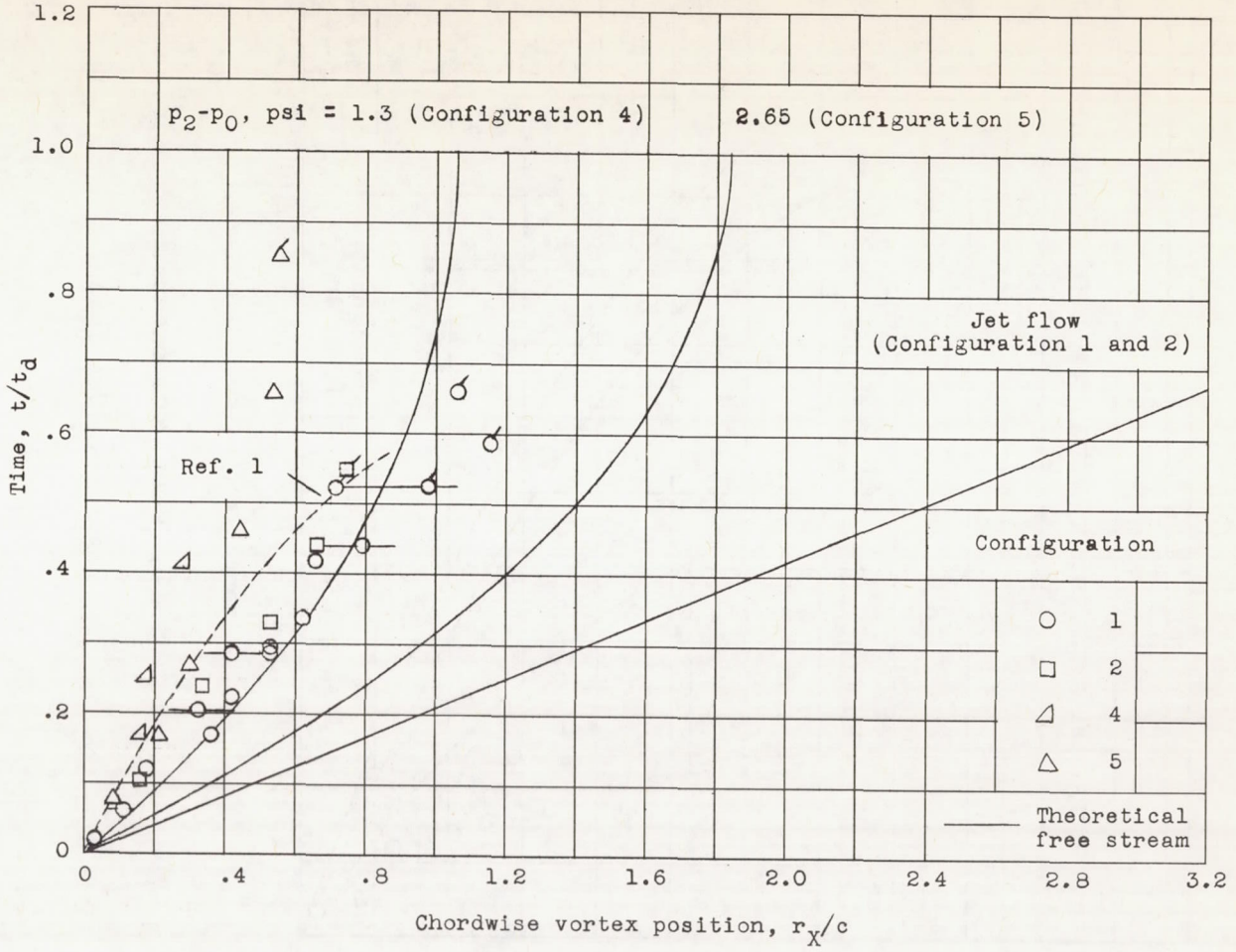

(a) Chordwise components.

Figure 8.- Leading-edge vortex position as a function of time. Flags indicate data taken after wave reflections.

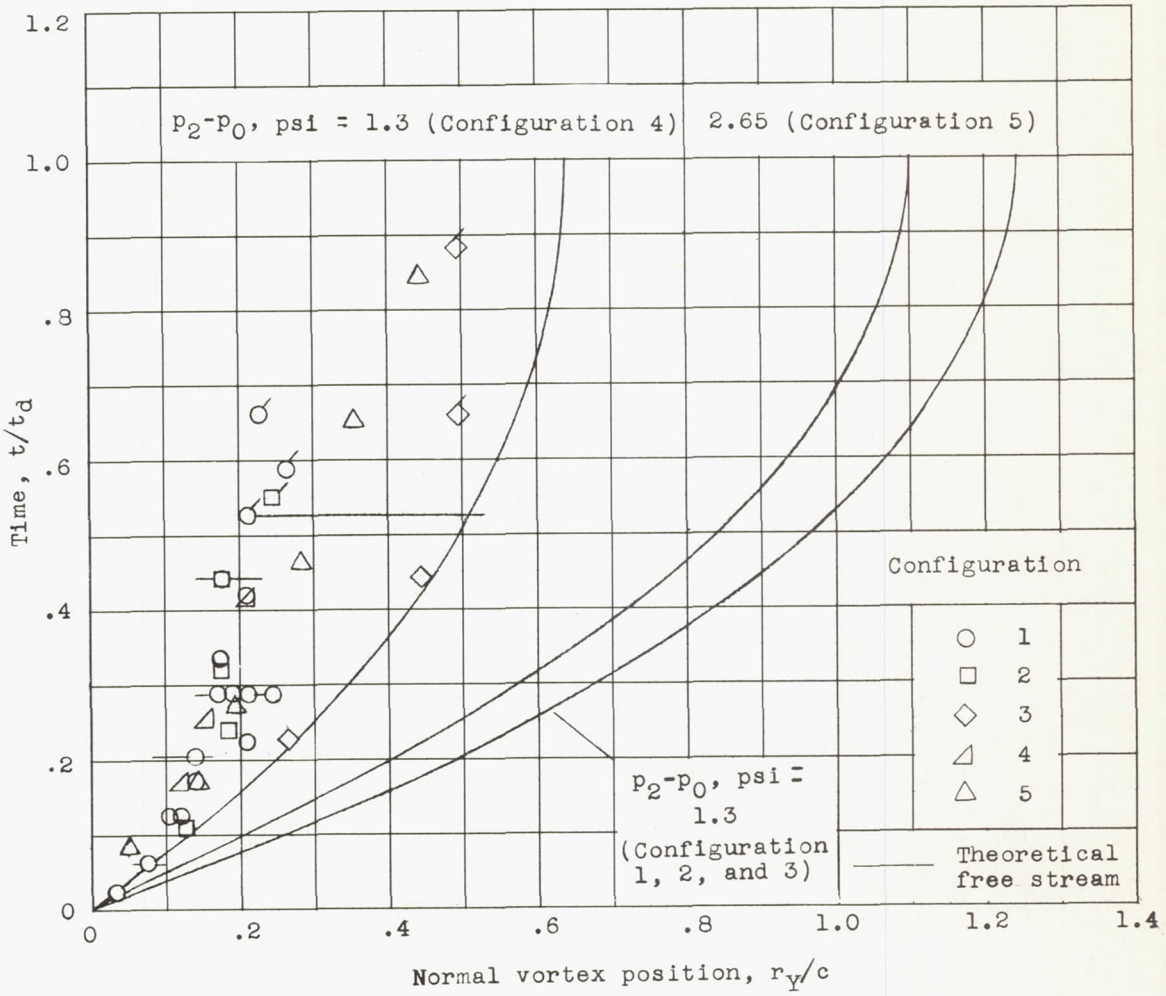

(b) Normal components.

Figure 8.- Concluded.

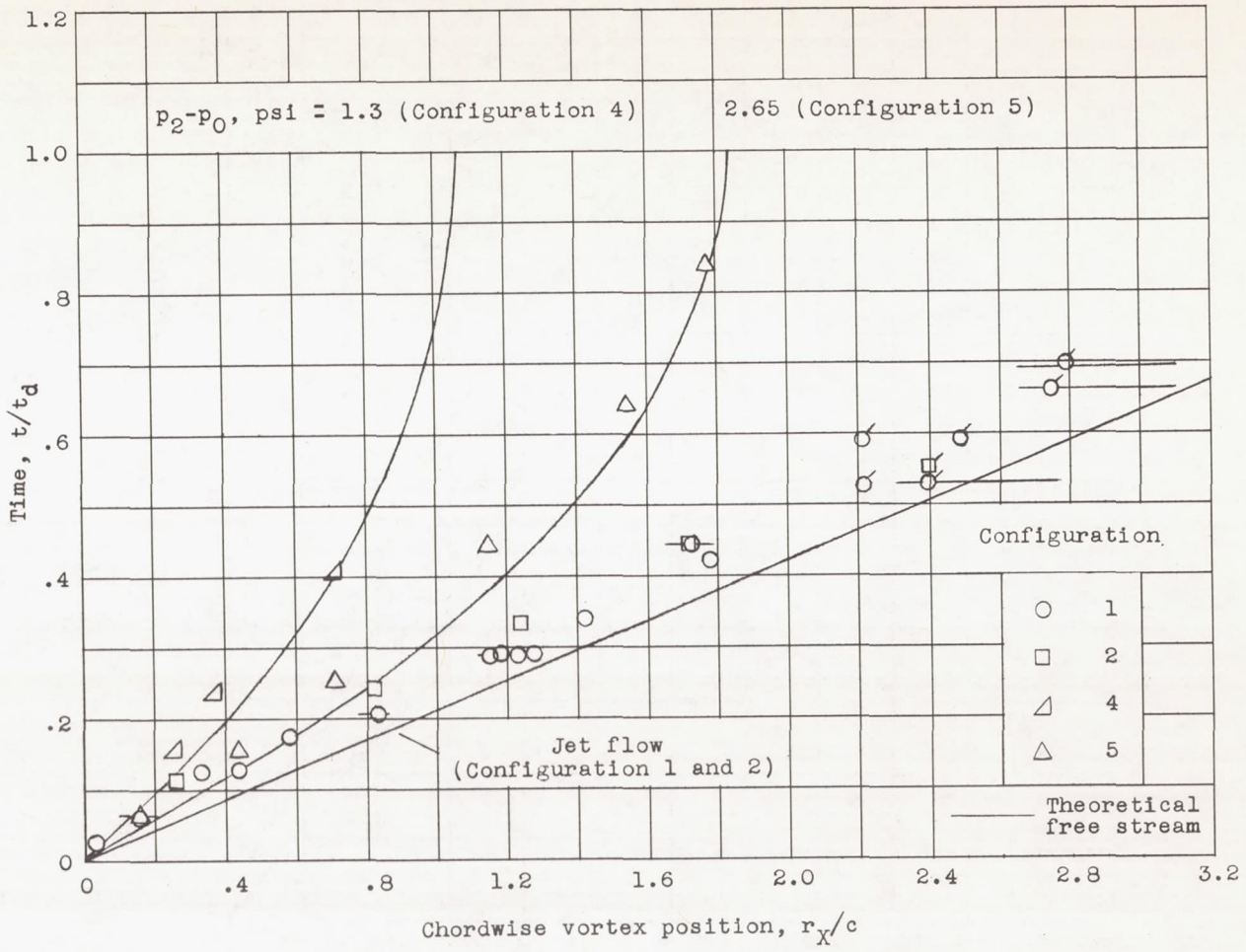

(a) Chordwise components.

Figure 9.- Trailing-edge-vortex position as a function of time. Flags indicate data taken after wave relections.

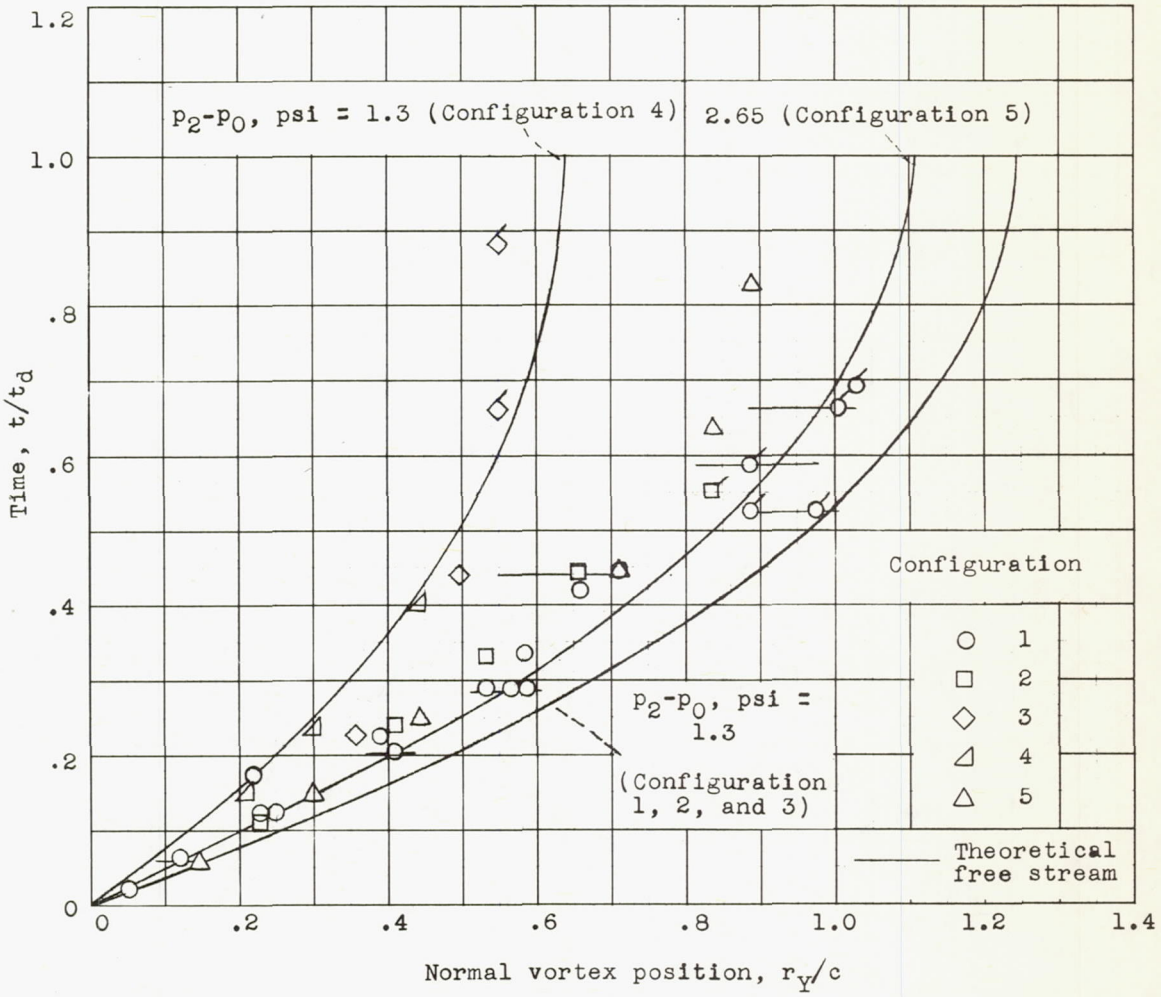

(b) Normal components.

Figure 9.- Concluded.

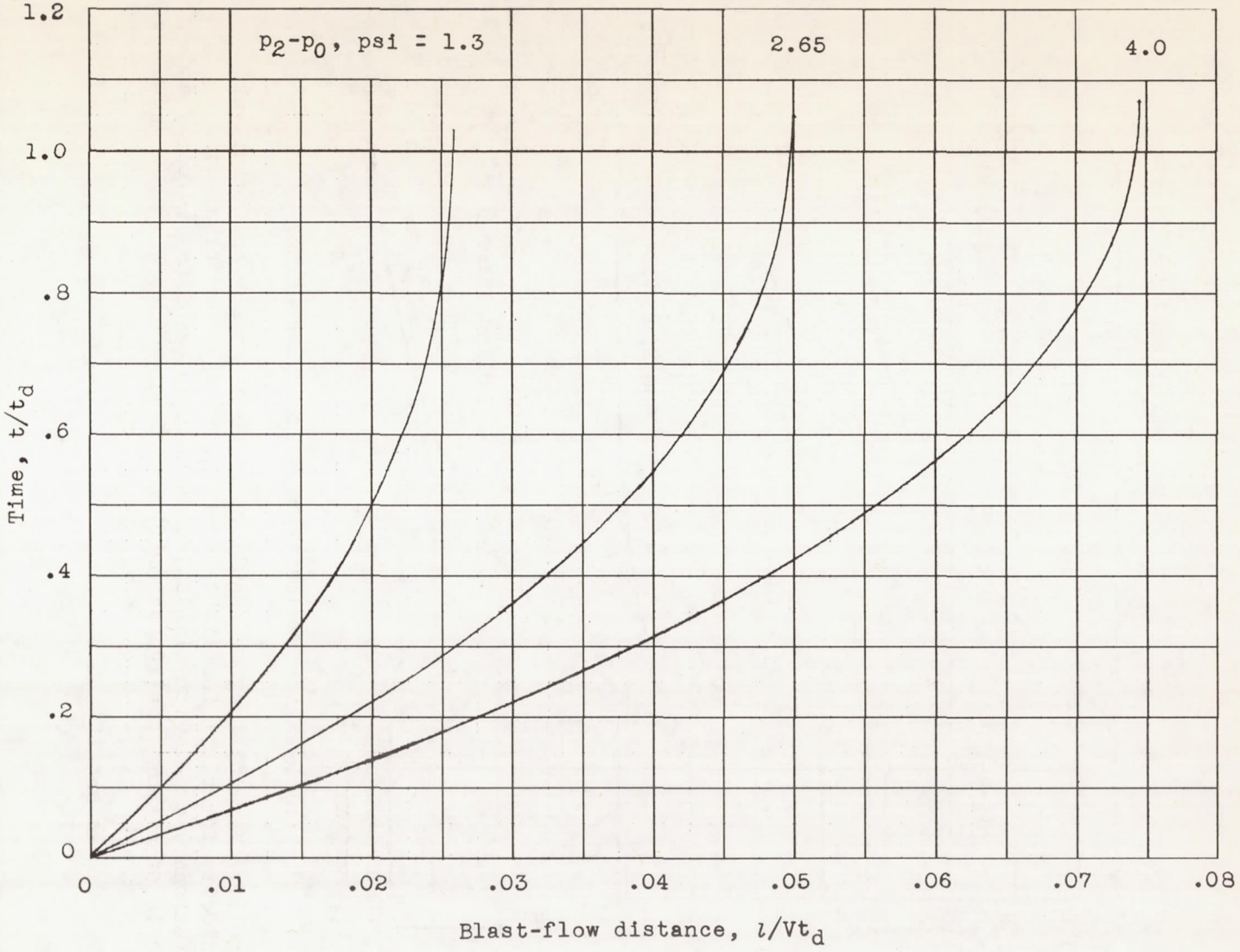

Figure 10.- Nondimensional variation of blast-flow distance with time.

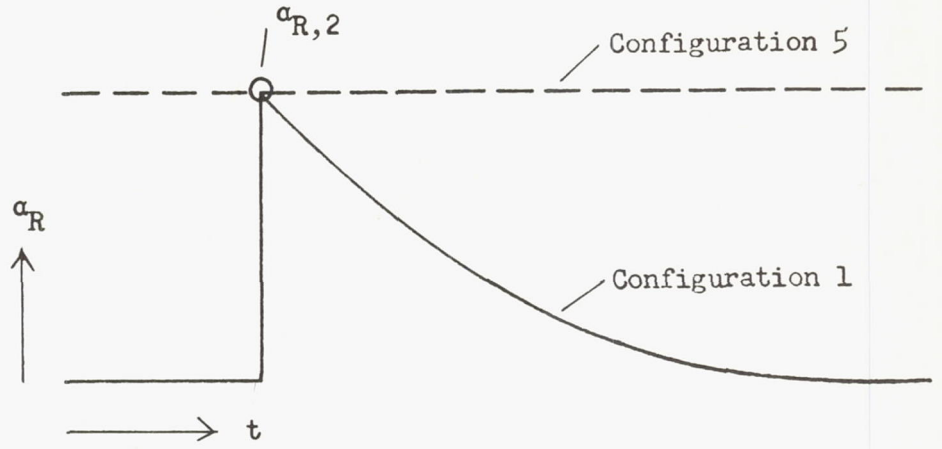

(a) Angle of attack plotted against time.

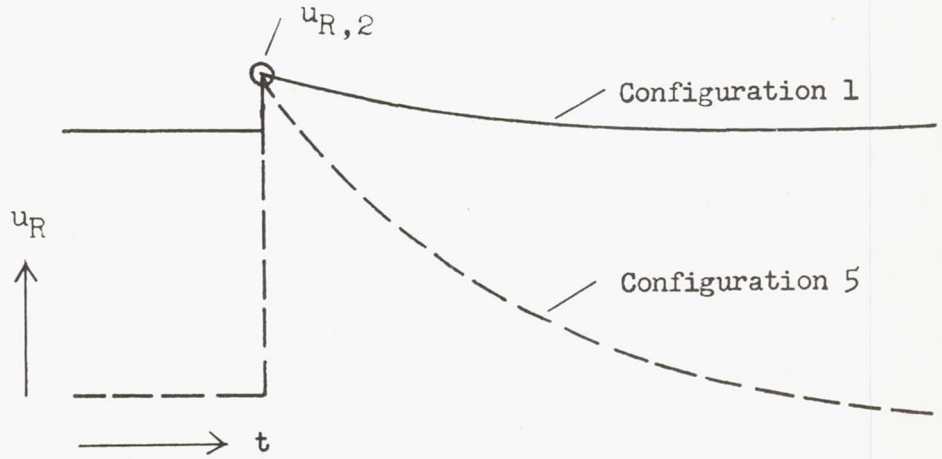

(b) Resultant velocity plotted against time.

Figure 11.- Time history of resultant angle of attack and resultant velocity for blast in flight (configuration 1) and blast over stationary model with simulation of maximum resultant velocity and angle of attack (configuration 5).

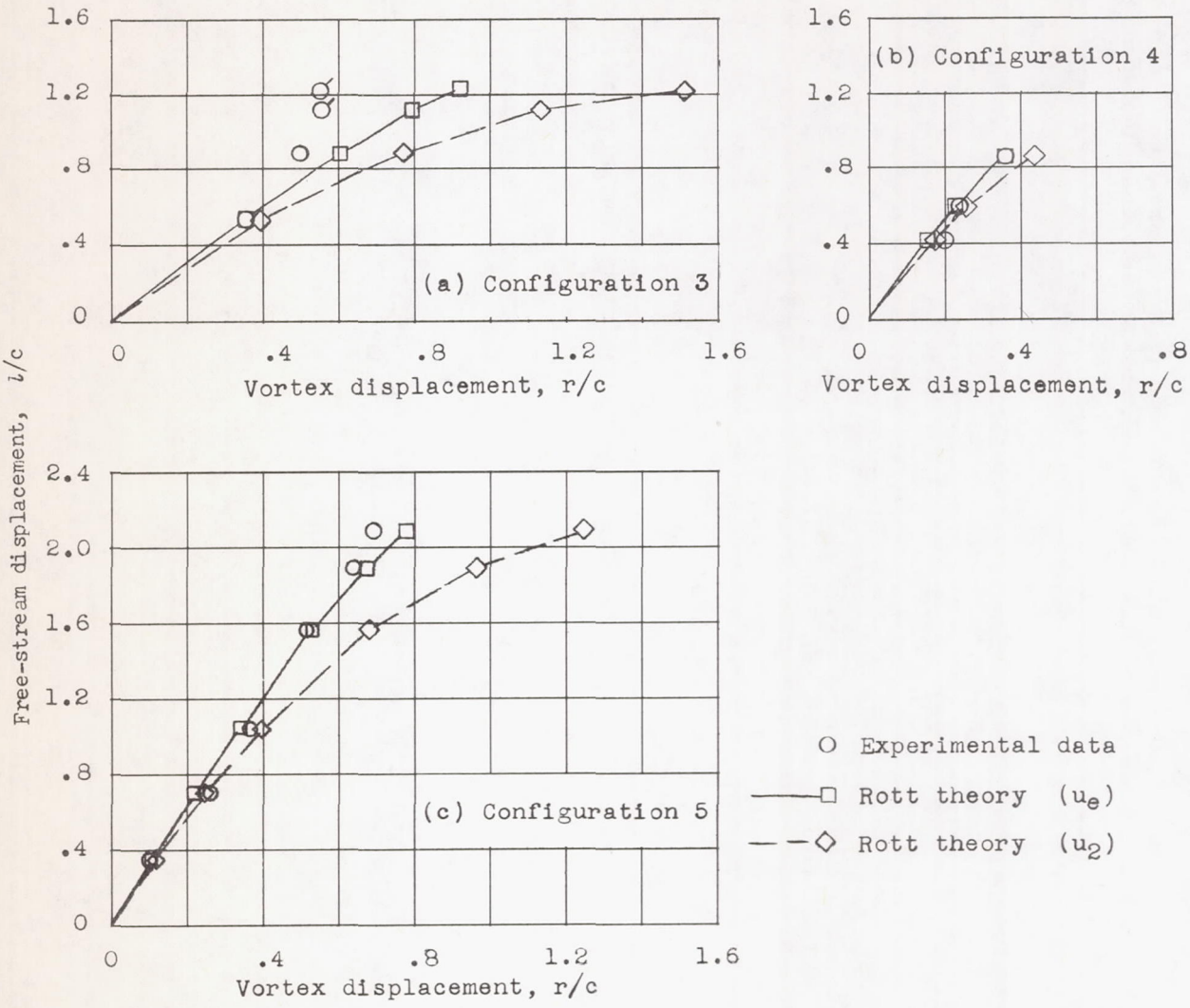

Figure 12.- Comparison of vortex displacement with Rott theory. Flags indicate data after wave reflections.